Science Advances
AAAS

Supplementary Materials for

Toxoplasma gondii macrophage migration inhibitory factor shows anti–*Mycobacterium tuberculosis* potential via AZIN1/STAT1 interaction

Chanjin Yoon *et al.*

Corresponding author: Chul-Su Yang, chulsuyang@hanyang.ac.kr

Sci. Adv. **10**, eadq0101 (2024)
DOI: 10.1126/sciadv.adq0101

This PDF file includes:

Supplemental information

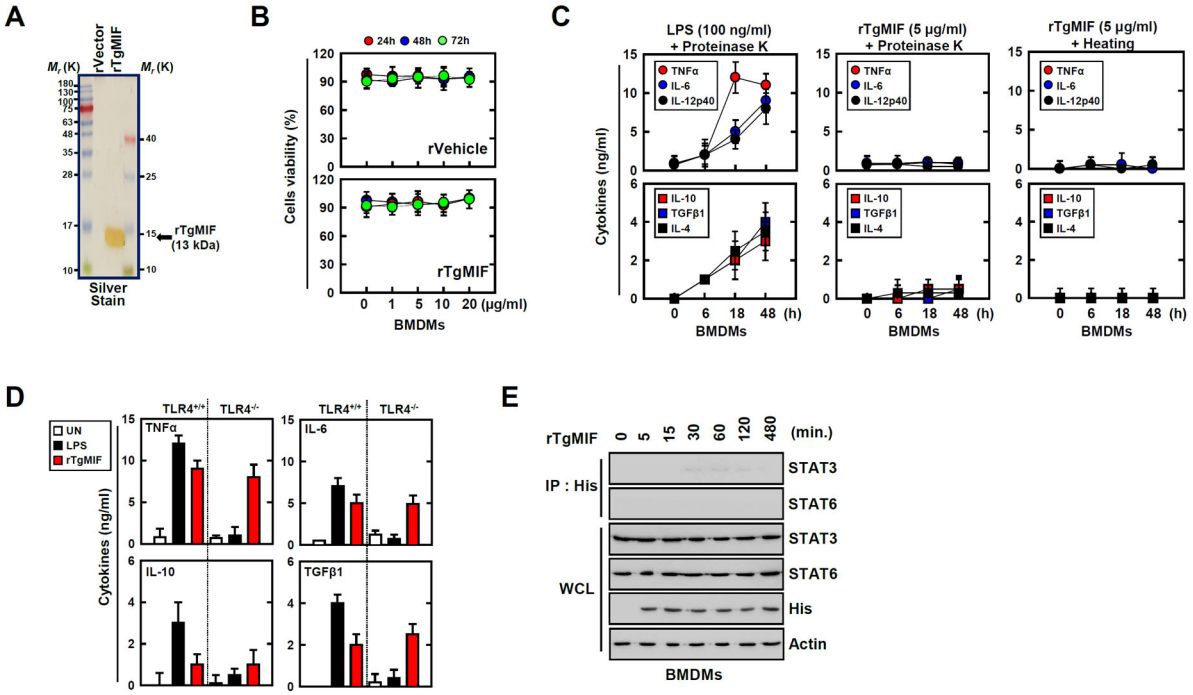

Figure S1. TgMIF establishment and validation in BMDMs. (A) Bacterially purified 6xHis-TgMIF validation through silver staining. (B) Evaluation of cytotoxicity induced by pTgMIF in BMDMs. The data shown are the means ± SD of five experiments. (C) Expression of pro-inflammatory cytokines (TNF-α, IL-6, and IL-12p40) and anti-inflammatory cytokines (IL-10, TGF-β1, and IL-4) in BMDMs treated with rTgMIF (5 μg/mL) with proteinase K or heating. The data shown are the means ± SD of five experiments. (D) BMDMs from $TLR4^{+/+}$ and $TLR4^{+/+}$ treated with LPS (100 ng/ml) or rTgMIF (5 μg/mL) for 24 h. Cell culture supernatants were analyzed for cytokine detection of TNF-α, IL-6, IL-10 and TGF-β. The data shown are the means ± SD of five experiments. (E) Interaction specificity of TgMIF with endogenous CD74, STAT1, or AZIN1 in stimulated BMDMs. The data are representative of four independent experiments with similar results. Full-length images of the blots presented in the Figure S8.

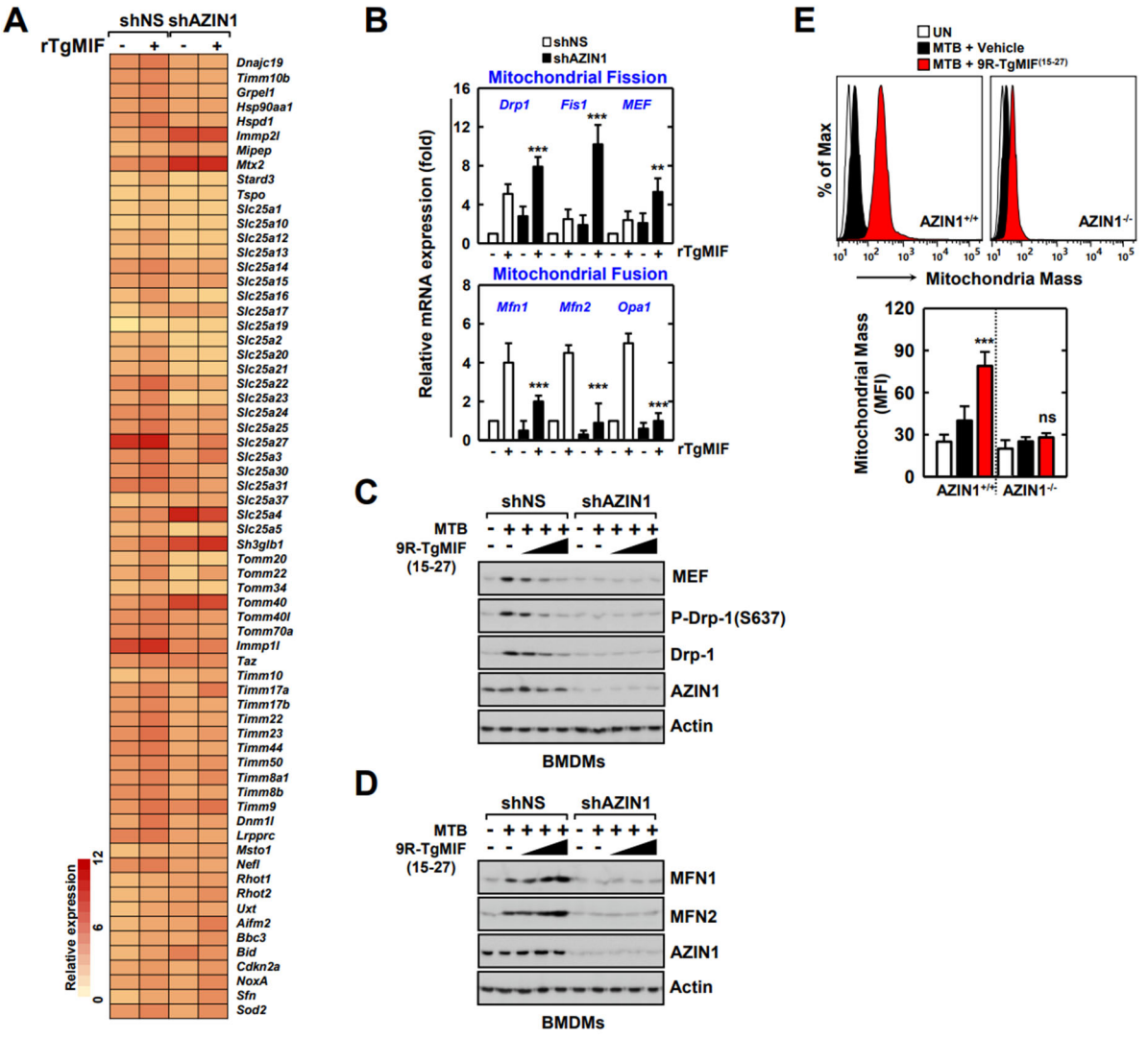

Figure S2. TgMIF modulates mitochondrial fusion and fission through AZIN1. (A) Regulation of mitochondrial dynamics by TgMIF in association with AZIN1 through DGE analysis. (B–D) Expression levels of genes involved in mitochondrial fission (DRP1, FIS1, MEF) and fusion (MFN1, MFN2, OPA1) by AZIN1 in BMDMs treated with rTgMIF. The data are representative of four independent experiments with similar results (C and D). (E) AZIN1-dependent TgMIF mitochondrial mass regulation in MTB-infected macrophages. Statistical significance was determined by the Student's t-test with Bonferroni adjustment (*P <0.05; **P <0.01; ***P <0.001). Full-length images of the blots presented in the Figure S8.

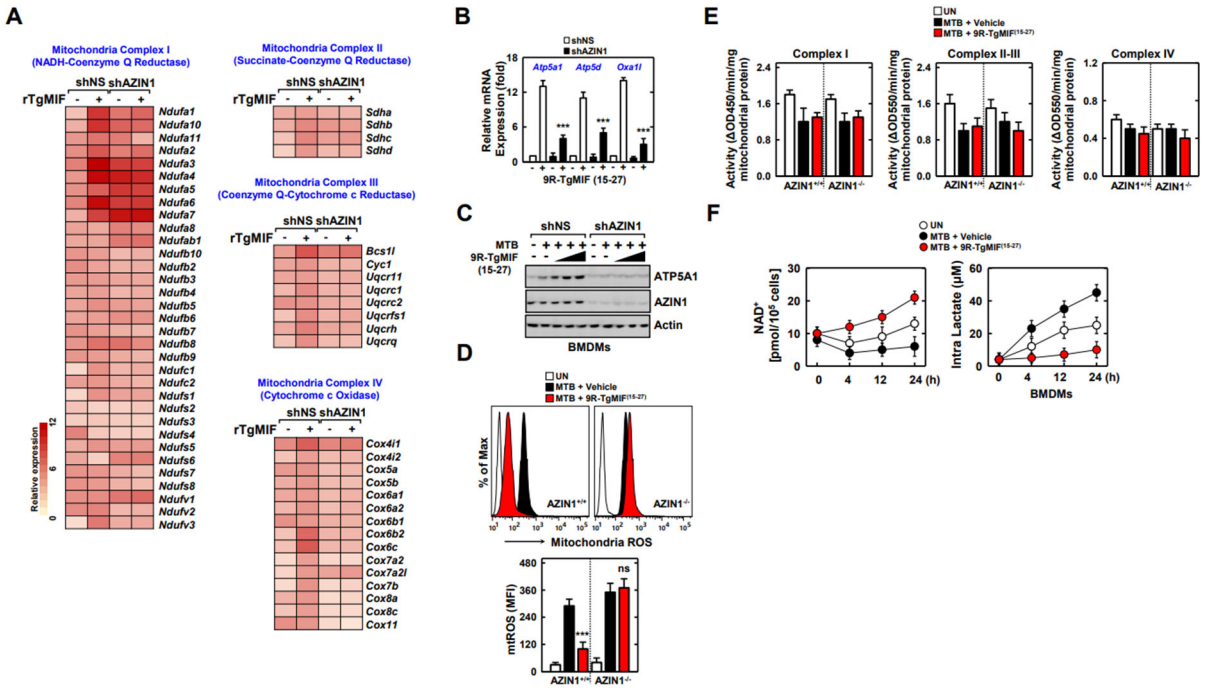

Figure S3. Modulation of mitochondrial complex V activity by TgMIF through AZIN1. (A) Analysis of differentially expressed genes (DEGs) involved in mitochondrial complexes affected by TgMIF and AZIN1. (B and C) Regulation of genes related to mitochondrial ATP synthase by AZIN1 in BMDMs treated with rTgMIF. The data are representative of four independent experiments with similar results. (D) ROS regulation in MTB-infected macrophages treated with TgMIF is dependent on AZIN1 expression. (E) Specific modulation of mitochondrial complex V activity by TgMIF, influenced by AZIN1. (F) Metabolic regulation through alterations in NAD+ and intracellular lactate levels by TgMIF, depending on AZIN1. The data shown are the means ± SD of five experiments. Full-length images of the blots presented in the Figure S8.

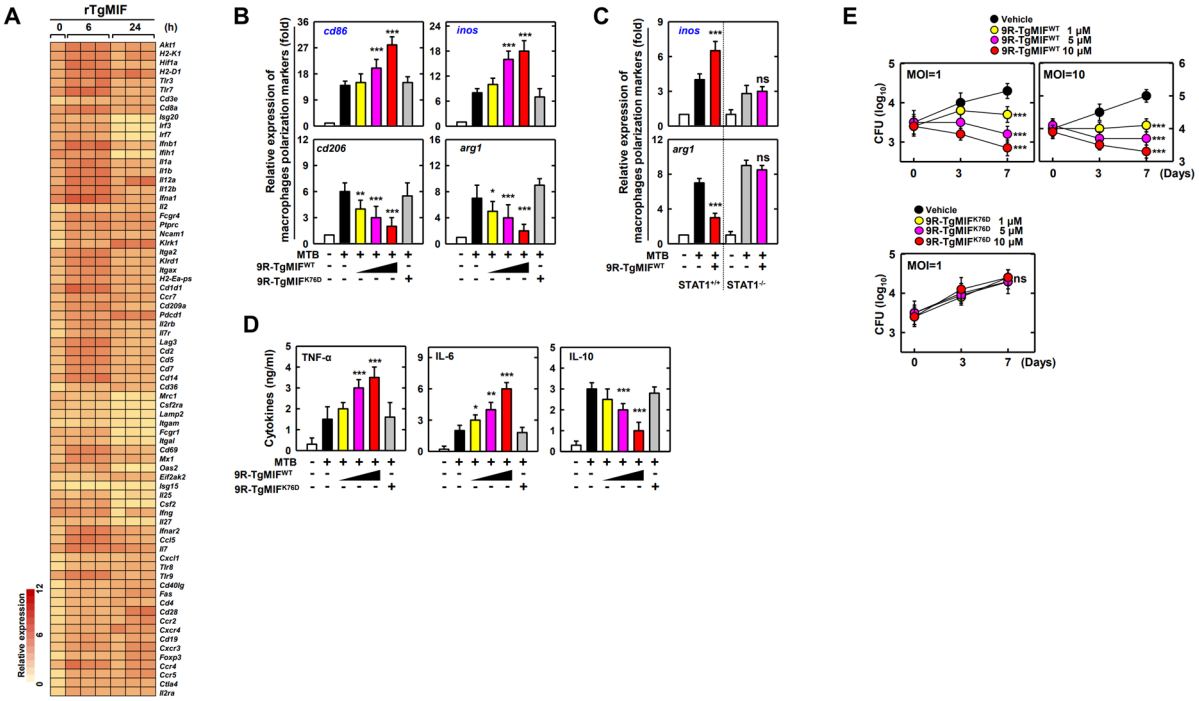

Figure S4. Effects of TgMIF on Macrophage Response to MTB Infection. (A) Differential expression patterns of candidate genes in response to TgMIF treatment. (B) Alteration in macrophage polarization markers upon TgMIF treatment in MTB-infected macrophages. (C) STAT1-dependency of macrophage polarization by TgMIF in MTB-infected macrophages (D) Effect of TgMIF on inflammatory cytokine production in MTB-infected macrophages. (E) Inhibition of MTB growth by STAT1-dependent TgMIF for the indicated dose and MOI. Statistical significance was determined by the Student's t-test with Bonferroni adjustment (**P* <0.05; ***P* <0.01; ****P* <0.001).

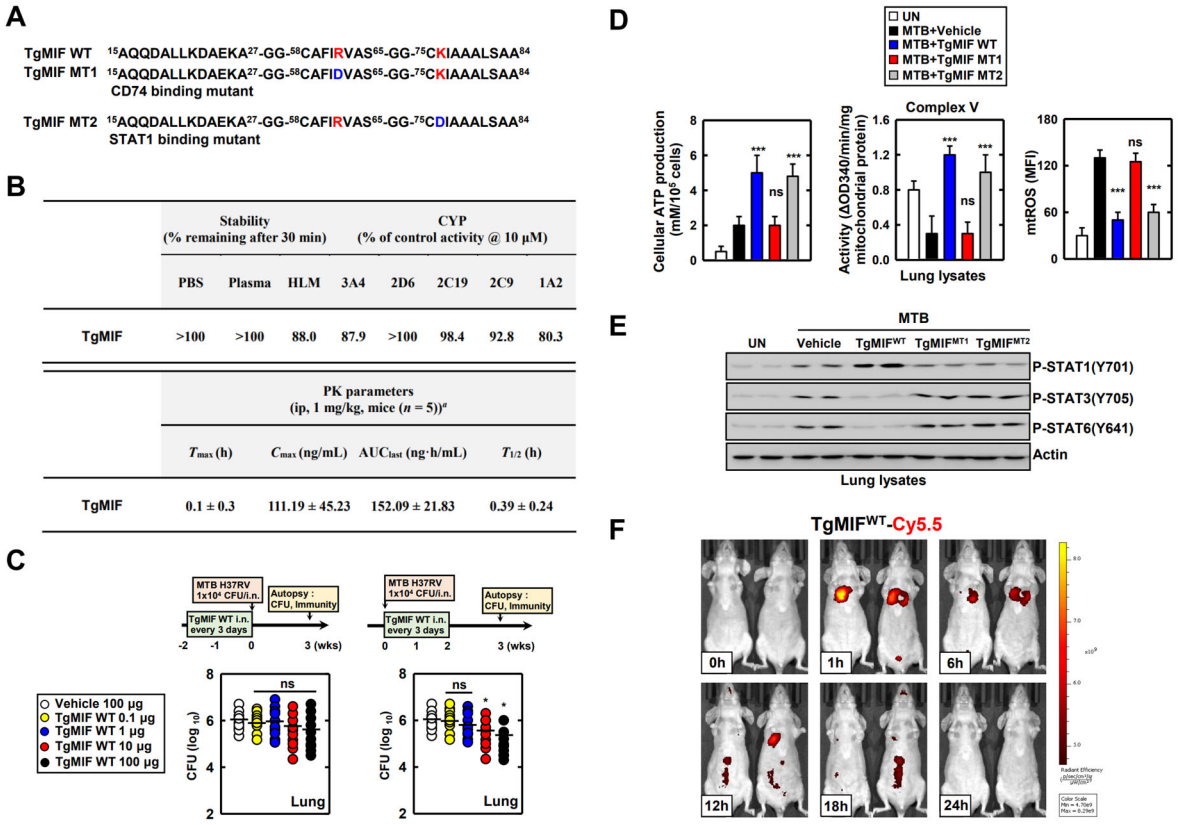

Figure S5. Experimental characterization of TgMIF peptide mutants. (A) Design of TgMIF peptide mutants targeting CD74 and STAT1. (B) Assessment of peptide stability, CYP enzyme metabolism, and PK parameters. (C) Optimal timeline design for MTB inhibition using TgMIF. (D) Effect of TgMIF on mitochondrial function in MTB-infected mice. (E) Specific modulation of STAT1 phosphorylation by TgMIF. (F) *In vivo* bio-distribution analysis by IVIS imaging of TgMIF^{wt}-Cy5.5 at various predetermined periods after MTB infection. Statistical significance was determined by the Student's t-test with Bonferroni adjustment (*P <0.05; **P <0.01; ***P <0.001). Full-length images of the blots presented in the Figure S8.

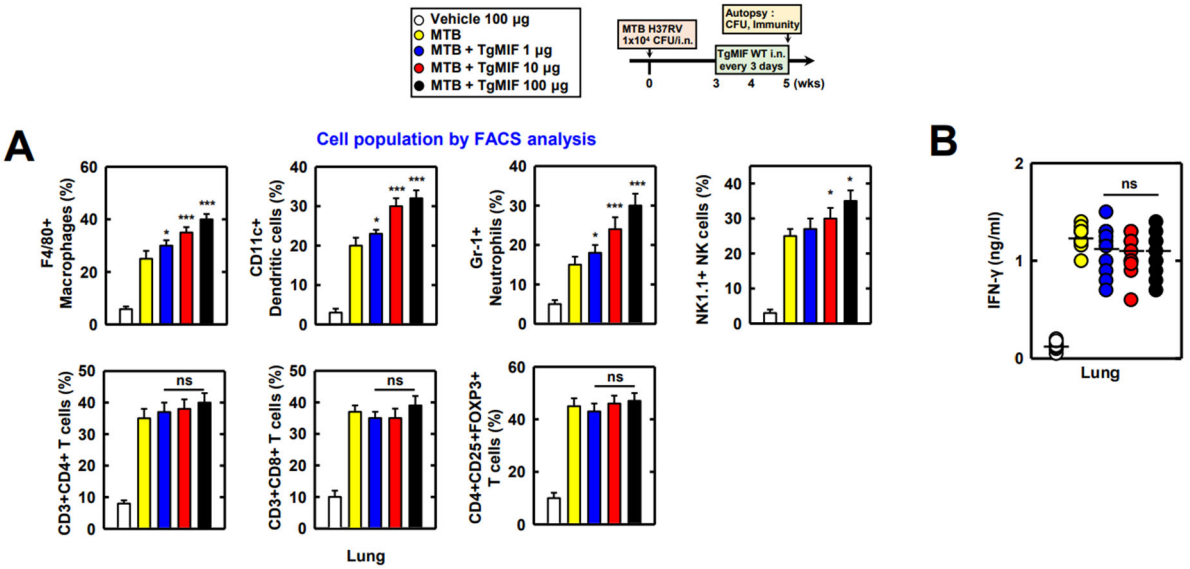

Figure S6. Immune cell population alterations and inflammatory cytokine modulation in the lungs of MTB-infected mice. (A) Alteration in immune cell populations in the lungs of MTB-infected mice. (B) TgMIF-driven modulation of inflammatory cytokine production in the lungs of MTB-infected mice. Statistical significance was determined by the Student's t-test with Bonferroni adjustment (**P* <0.05; ***P* <0.01; ****P* <0.001).

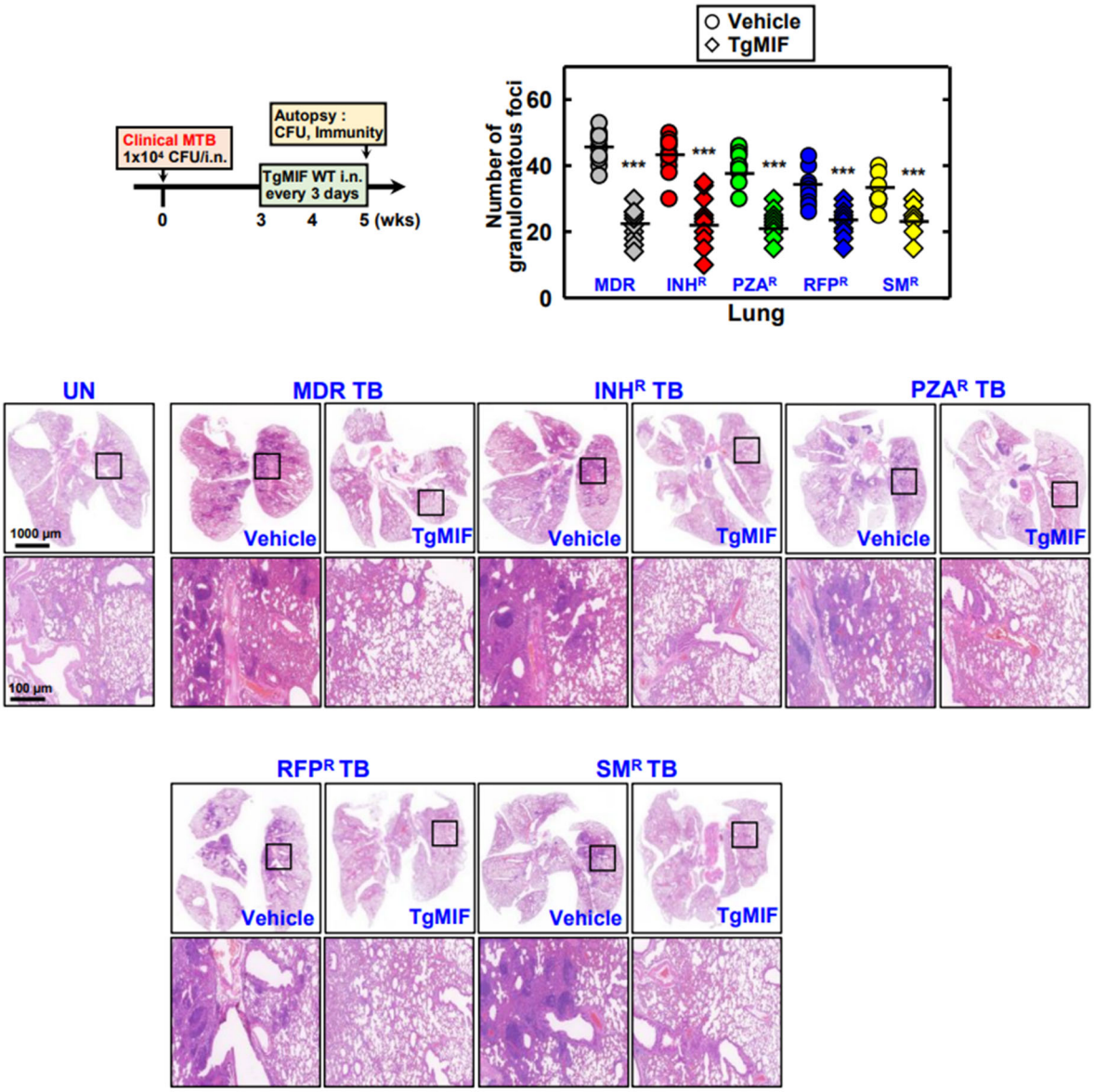

Figure S7. Effect of TgMIF on immune cell infiltration and lung damage in drug-resistant TB. Reduction of drug-resistant MTB-induced immune cell infiltration and lung damage through TgMIF post-treatment. Statistical significance was determined by the Student's t-test with Bonferroni adjustment (**P* <0.05; ***P* <0.01; ****P* <0.001).

Figure S8 Full-length images of the blots presented in the Figures.

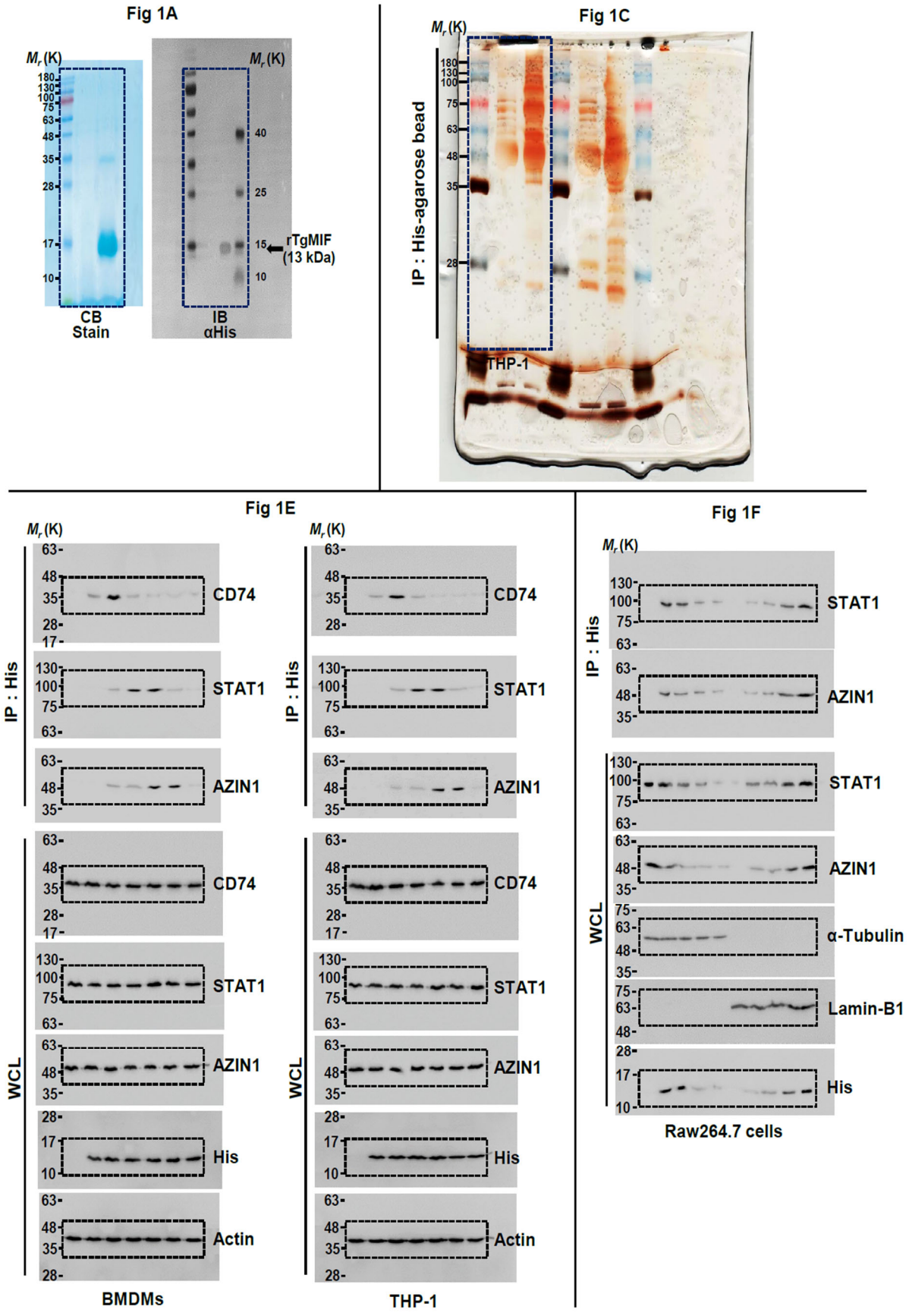

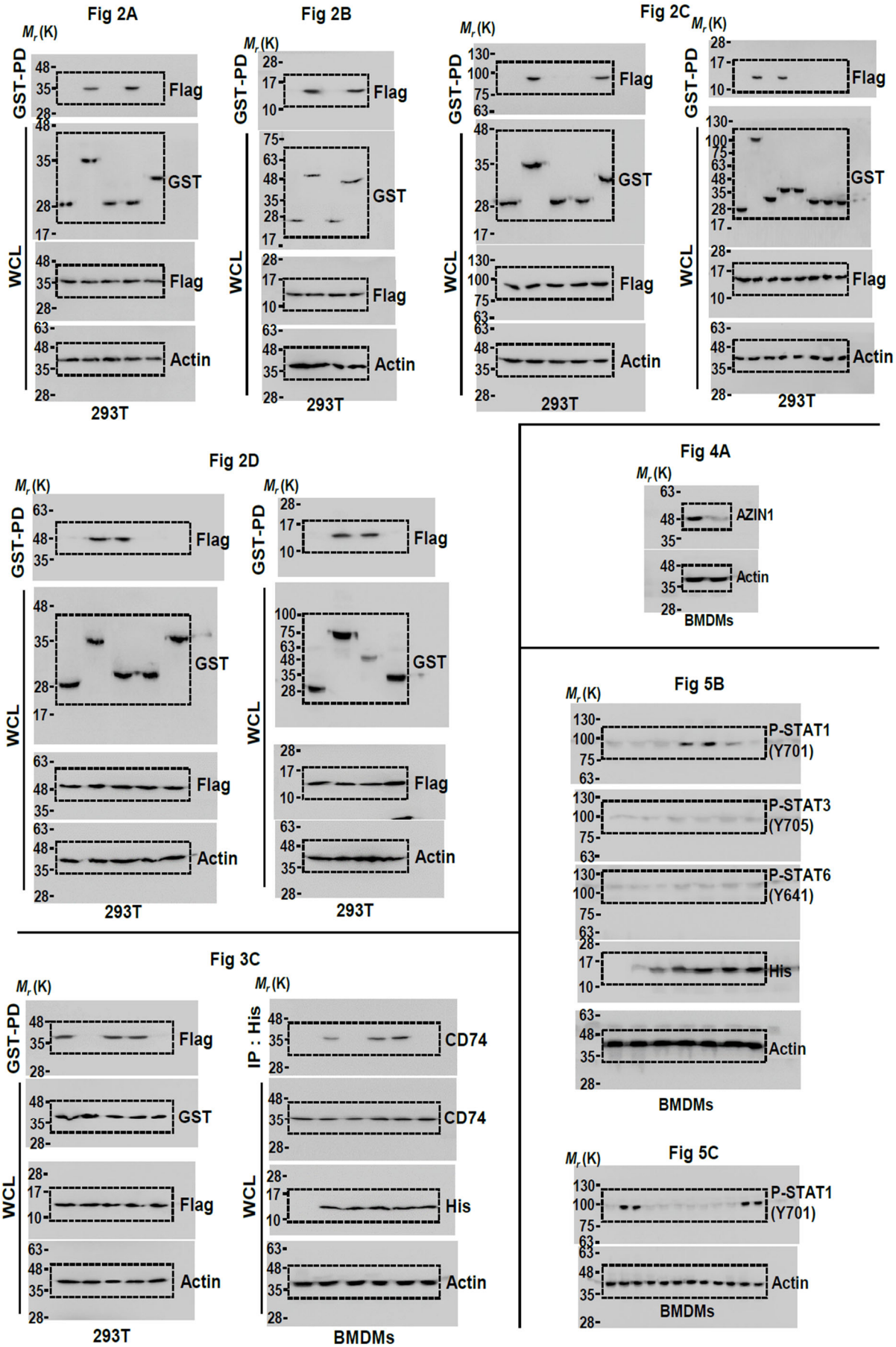
Fig 2A
Fig 2B
Fig 2C
Fig 2D
Fig 3C
Fig 4A
Fig 5B
Fig 5C
M_r(K)
GST-PD
WCL
Flag
GST
Actin
293T
IP : His
CD74
His
AZIN1
BMDMs
P-STAT1 (Y701)
P-STAT3 (Y705)
P-STAT6 (Y641)

Fig S1A

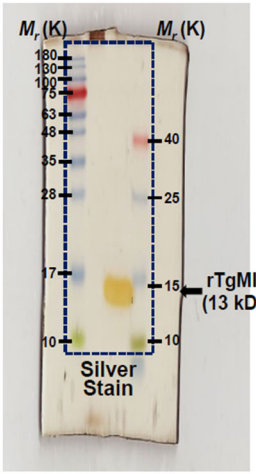

Fig S1C

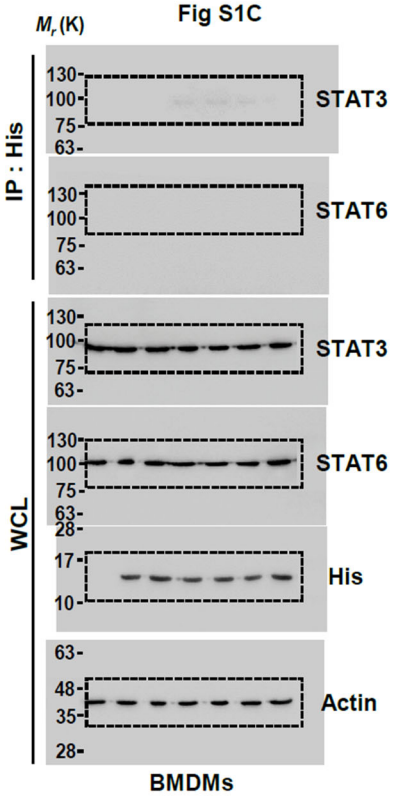

Fig S3C

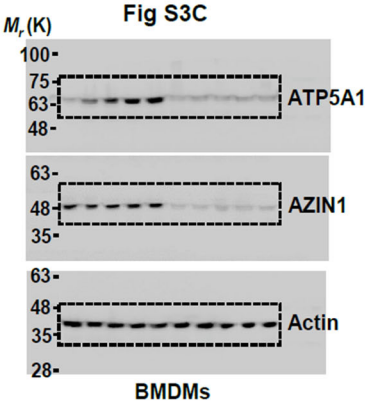

Fig S2C

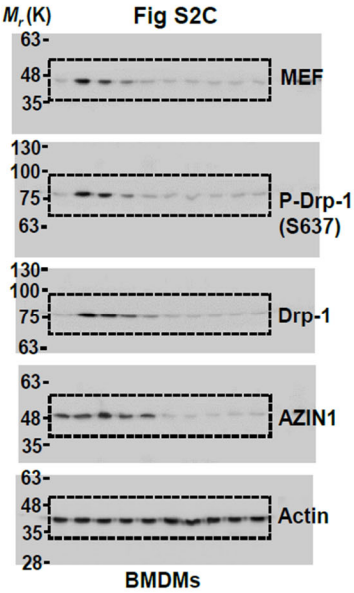

Fig S2D

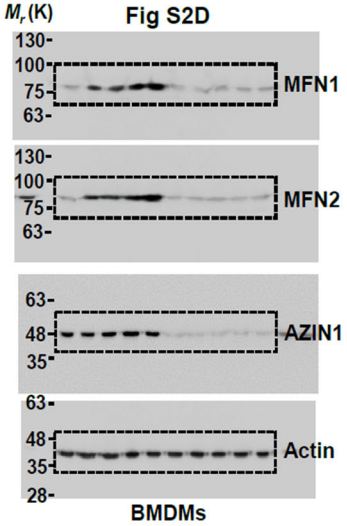

Fig S5E

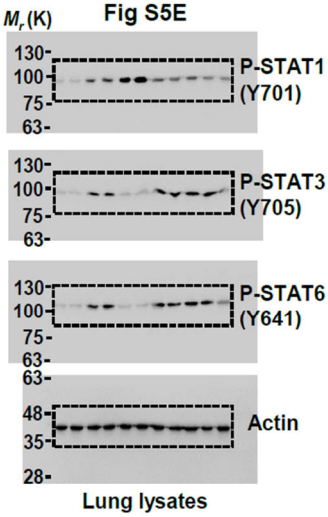

Supplemental Experimental Procedures

Recombinant protein

To obtain *T. gondii* ME49 strain-derived MIF (GenBank accession no. XP_002368429.1) recombinant protein, the MIF amino acid (1–116) sequence was cloned with an N-terminal 6xHis tag into the pRSFDuet-1 vector (Novagen), induced, harvested, and purified from *Escherichia coli* expression strain BL21(DE3)pLysS, as described previously, (25) following the standard protocols recommended by Novagen.

For biological assays, rTgMIF was dialyzed with a permeable cellulose membrane, endotoxin was removed from protein samples using the ProteoSpin Endotoxin Removal Maxi kit (Novagen), and tested for lipopolysaccharide contamination with a *Limulus Amebocyte Lysate* (LAL) assay (Lonza Inc., Basel, Switzerland) according to the manufacturer's instructions. The experiments and data analysis were performed by using an ELx808 microplate reader (BioTek, Winooski, VT, USA) equipped with WinKQCL version 5.3.3. software (Lonza Inc., Walkersville, MD, USA) and contained < 10 pg/mL of the rTgMIF proteins used in the experiments described here.

Characterization of endotoxin-free TgMIF

To assess whether the rTgMIF activity is protein-based, heating and/or proteinase-k digestion were used to degrade protein components in rTgMIF. (1) rTgMIF added to the proteinase-K (Sigma-Aldrich), incubated at 37 °C for 80 min (shaken every 10 min), centrifuged at 4,000 rpm for 1 min, and supernatant was frozen at −80 °C. (2) Heating was performed at 80 °C for 15 min in a water bath (VWR Scientific, West Chester, PA, USA) after which the medium was centrifuged for 10 min at 10,000 rpm, 4 °C to separate out the denatured proteins, and supernatant was

frozen at −80 °C. (3) BMDMs from $TLR4^{+/+}$ and $TLR4^{-/-}$ treated with rTgMIF. $TLR4^{-/-}$ mice were a generous gift from Dr. Chul-Ho Lee (Laboratory Animal Center, Korea Research Institute of Bioscience and Biotechnology, Daejeon, Korea).

Protein purification and mass spectrometry

To identify TgMIF-binding proteins, THP-1 cells treated with rTgMIF were harvested and lysed with NP-40 buffer (50 mM HEPES, pH 7.4, 150 mM NaCl, 1 mM EDTA, and 1% (v/v) NP40) supplemented with a complete protease inhibitor cocktail (Roche). Post-centrifuged supernatants were pre-cleared with protein A/G beads at 4°C for 2 h. Pre-cleared lysates were mixed with αFlag antibody conjugated with agarose beads for 4 h at 4°C. The precipitate was washed extensively with the lysis buffer. Proteins bound to the beads were eluted and separated on a Nupage 4–12% Bis-Tris gradient gel (Invitrogen). After silver staining (Invitrogen), specific protein bands were excised and analyzed using ion-trap mass spectrometry at the Korea Basic Science Institute Mass Spectrometry facility. Amino acid sequences were determined by tandem mass spectrometry and database searches.

Flow Cytometry, data Analysis and gating principle

For analysis in endocytosis pathway of TgMIF (**Fig. 3A**), rTgMIF was conjugated with Texas Red using the Texas Red® Conjugation Kit (Fast)-Lightning-Link (Abcam) to quantitatively measure the cellular uptake of macrophages. The cells were quickly and thoroughly washed with a pulse spin and immediately analyzed samples were acquired on the conventional flow cytometer BD FACSymphony (BD Biosciences, San Jose, CA, USA) and analyzed with BD FACSDiva software (Version

8.0.01, BD Biosciences). The obtained data were analyzed using FlowJo software (Version 10.7.1, BD Biosciences). Different subpopulations were identified based on a standard flow cytometry gating strategy. Like in conventional flow cytometry, on both systems, we excluded debris and doublets based on forward and sideward scatter information. Next, dead cells were excluded based on viability staining.

For analysis of immune cell populations in the lungs of MTB-infected mice (**Fig. S6A**)**,** (*Top*) Myeloid cells were stained with F4/80-PE (Clone. W20065D, Cat. No. 111703), CD11c-PE (Clone. N418, Cat. No. 117307), Ly-6G/Ly-6C (Gr-1)-PE (Clone. RB6-8C5, Cat. No. 108407), NK-1.1-PE (Clone. S17016D, Cat. No. 156503) and DAPI to identify viable cells. Cells were gated for Macrophages (F4/80), Dendritic cells (CD11c), Neutrophil (Gr-1), NK and (NK1.1) based on side scatter area and viable cells in the population of lung lysates was calculated. (*Bottom*) T cells were stained with CD3-PE (Clone. 17A2, Cat. No. 100205), CD4-PE (Clone. GK1.5, Cat. No. 100407), CD8-PE (Clone. YTS156.7.7, Cat. No. 126607), CD25-FITC (Clone. 3C7, Cat. No. 101907) and DAPI to identify viable. Based on this subpopulation, we selected the total $CD3^+$ population (versus side scatter) and subsequently selected all $CD3^+CD4^+$ or $CD3^+CD8^+$ cells based on uninfected controls. From the same viable $CD3^+$ population, we also gated all $CD3^+CD4^+$ versus $CD3^+CD4^-$ cells and $CD3^+CD8^+$ versus $CD3^+CD8^-$ cells. We selected the total $CD4^+$ population (versus side scatter) and subsequently selected all $CD4^+CD25^+$ cells based on uninfected controls. From the same viable $CD4^+$ population, we also gated all $CD4^+CD25^+$ versus $CD4^+CD25^-$ cells. Both cell populations were subsequently gated for their $DAPI^-$ cells based on uninfected controls. Antibodies specific for FACS analysis were purchased from BioLegend (BioLegend, Inc., San Diego, CA, USA).

In vivo imaging

TgMIF-Cy5.5 was prepared by adding streptavidin-conjugated Cy5.5 dye to the TgMIF-WT peptide. TgMIF-Cy5.5 was administered to MTB-infected mice. To study tissue biodistribution, mice were sacrificed at different time points post-administration, and major organs were excised and imaged using the IVIS Spectrum-CT *in vivo* imaging system (PerkinElmer, Inc.).